

Francisite, $\text{Cu}_3\text{Bi}(\text{SeO}_3)_2\text{O}_2\text{Cl}$, a new mineral from Iron Monarch, South Australia: Description and crystal structure

ALLAN PRING

Department of Mineralogy, South Australian Museum, North Terrace, Adelaide, South Australia 5000, Australia

BRYAN M. GATEHOUSE

Department of Chemistry, Monash University, Clayton, Victoria 3168, Australia

WILLIAM D. BIRCH

Department of Mineralogy and Petrology, Museum of Victoria, 285 Russell Street, Melbourne, Victoria 3000, Australia

ABSTRACT

Francisite is a new copper bismuth oxy-chloro selenite from Iron Monarch, South Australia. The new mineral occurs as radiating clusters of bright green bladed crystals up to 0.25 mm in length. The crystals are elongated along [010], and the principal forms are {100}, {011}, and {101}. Associated with francisite are barite, chlorargyrite, muscovite, native bismuth, naumannite, djurleite, and a number of poorly characterized selenides of Bi, Ag, and Cu. Francisite appears to have formed as a result of hydrothermal alteration of the selenide and sulfide minerals.

Electron microprobe analysis yielded CuO 32.62, Bi_2O_3 35.75, SeO_2 27.23, Cl 4.11, less O = Cl, 0.93, total 98.78 wt%; the simplified formula is close to $\text{Cu}_3\text{Bi}(\text{SeO}_3)_2\text{O}_2\text{Cl}$. The mineral is transparent and has a pale green streak. The estimated Mohs hardness is 3–4, and $D_{\text{calc}} = 5.42 \text{ gm/cm}^3$. Single-crystal studies gave an orthorhombic cell with $a = 6.354(1)$, $b = 9.630(1)$, $c = 7.220(2) \text{ \AA}$, $V = 441.80(2) \text{ \AA}^3$, space group $Pmmn$ and $Z = 2$. The crystal structure was solved by Patterson methods and refined to $R = 0.0443$ and $wR = 0.0395$, using a set of 734 reflections, of which 434 were considered to be observed [$I > 3\sigma(I)$]. The structure consists of an infinite three-dimensional framework of cations and O, containing eight-coordinate Bi^{3+} , square-planar Cu^{2+} , and three-coordinate Se^{4+} . The Cl ions and the Se lone pair electrons occupy tunnels parallel to [001].

The strongest lines in the X-ray powder pattern are (d_{obs} , I_{obs} , hkl) 5.31 (60) (110); 3.39 (100) (121); 2.866 (80) (130); 2.652 (70) (220); 2.491 (60) (221); 1.695 (35) (242); 1.588 (60) (332). The name is for Glyn Francis of Iron Knob, South Australia.

INTRODUCTION

In May 1987 Glyn Francis, Quality Control Officer at the Iron Monarch iron deposit, submitted a group of specimens from the mine to one of us (A.P.) for identification. One specimen contained small bright apple green crystals that were unfamiliar. Energy-dispersive X-ray analyses showed that the mineral contained Cu, Bi, Se, and Cl, an unusual combination of elements. Electron microprobe and powder X-ray diffraction analyses indicated that the mineral was an undescribed species but left aspects of the mineral's chemistry unclear. A single-crystal structure determination was undertaken in order to fully resolve the composition and stoichiometry of the mineral. Francisite is a copper bismuth oxy-chloro selenite and has been named in recognition of Glyn Francis's contribution to the understanding and preservation of the minerals of the Iron Monarch ore body. The mineral and the name were approved by the Commission on New Minerals and Mineral Names in 1989. Type specimens are in the collections of the South Australian Museum, Adelaide, and the Museum of Victoria, Melbourne.

OCCURRENCE

The new mineral was found in cavities at the core of an isolated lens of barite within massive hematite ore on the 138-m level at the southern end of the open cut. The barite lens was at the lower end of an open channel running along the hinge of a major anticline within the ore body. In addition to barite, the minerals associated with francisite include chlorargyrite, which occurs as hexagonal prisms (pseudomorphs after apatite?) and fine-grained white muscovite. Also present are naumannite, native bismuth, djurleite, and several poorly defined copper, silver, and bismuth selenides, all of which occur as small blebs within the barite. Francisite occurs as radiating clusters and groups of bladelike crystals on barite crystals and in hollows in the fine-grained muscovite that fills many of the cavities within the barite. Approximately 100 small specimens bearing the new mineral were recovered; the total mass of francisite on all known specimens is <1 g.

Iron Monarch (32°45'S, 137°08'E) is a large sedimentary iron ore deposit of Precambrian age, situated in the

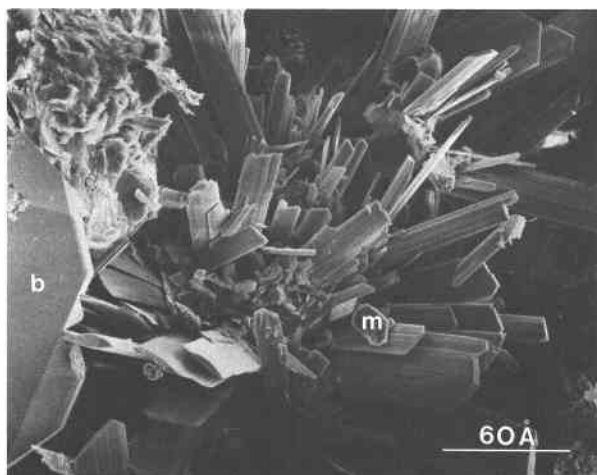


Fig. 1. SEM photomicrograph showing a group of francisite crystals, with a barite crystal (b) and flakes of muscovite (m).

Middleback Ranges of South Australia, approximately 400 km northwest of Adelaide. Iron Monarch and the adjoining deposit, Iron Knob, have been worked since the turn of the century by Broken Hill Proprietary Limited, first as a source of flux for the lead smelting works at Port Pirie and later as a source of iron ore for steel making. The principal ore mineral is hematite, which grades into siliceous banded iron formation (Milnes, 1954). The upper part of the deposit also contains large lenses of manganese oxides, principally hausmannite. Small amounts of other unusual secondary minerals, mainly phosphates, have also been found in isolated areas within the ore body (Segnit and Francis, 1983; Pring et al., 1989; Pilkington et al., 1979). The occurrence of francisite, native bismuth, and the associated selenide minerals is the first record of Se- and Bi-bearing minerals from Iron Monarch.

PHYSICAL AND OPTICAL PROPERTIES

Francisite occurs as bladed crystals up to 0.25 mm in length that are elongated parallel to [010]. The principal forms observed are {100}, {011}, and {101} (Figs. 1 and 2). Contact twinning on {100} is sometimes present. The crystals do not have a cleavage and when broken display a conchoidal fracture. Francisite is bright apple green in color (no. 140A on the Royal Horticultural Society of London chart) and the streak is a paler shade of apple green. The optical properties of francisite were not determined in detail, as the mineral was found to react with oils of high refractive index; all refractive indices were found to be greater than 1.79. The high refractive indices are in accord with the adamantine luster of the mineral. The crystals are length slow and exhibit a distinct pleochroism that varies in color from pale green to bright green, with the brighter shade being parallel to the length of the crystals. Neither the hardness nor the density could be accurately measured because of the small crystal size. The hardness is estimated at 3–4, and the crystals were

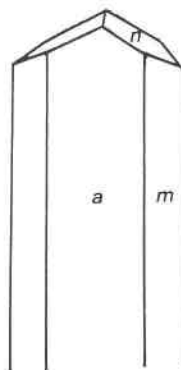


Fig. 2. Schematic diagram showing the principal forms of francisite: *a*, {100}; *m*, {101}; and *n*, {011}.

found to sink in Clerici's solution; the calculated density is 5.42 g/cm³.

CHEMISTRY

Francisite was analyzed using a JEOL electron microprobe operating at 15 kV with a specimen current of 0.020 μA . The standards used were pure metals (Cu, Bi), berzelianite (Se), and NaCl (Cl). No other elements with an atomic number greater than eight were detected by wavelength spectroscopy, and H₂O was not determined, as the infrared spectrum indicated that neither H₂O nor OH was present. A total of seven analyses were obtained, for which the average is given in Table 1. The empirical formula, calculated on the basis of nine anions, is $\text{Cu}_{3.10}\text{Bi}_{1.16}\text{Se}_{1.86}\text{O}_{8.12}\text{Cl}_{0.88}$, with the simplified formula being $\text{Cu}_3\text{Bi}(\text{SeO}_3)_2\text{O}_2\text{Cl}$. This formula was confirmed by the crystal structure determination.

POWDER X-RAY DIFFRACTION

The powder X-ray diffraction pattern was recorded using a 100-mm diameter Guinier-Hägg camera with monochromated $\text{CuK}\alpha_1$ radiation and with Si employed as an internal standard. Line intensities were estimated visually by comparison with a set of standard reflections. The powder pattern (Table 2) was indexed on an orthorhombic cell and, least-squares refinement was undertaken using 34 reflections with $2\theta < 80^\circ$. The final parameters obtained were $a = 6.356(1)$, $b = 9.633(2)$, $c = 7.224(2)$ Å.

INFRARED SPECTRUM

The infrared spectrum of francisite was recorded on a Mattson Instruments Cygnus 25B Fourier transform infrared spectrophotometer. The spectrum contains three absorption bands. Weak bands are present at 1000 cm^{-1} and 820 cm^{-1} , and a strong band is evident between 680 and 740 cm^{-1} . The strong band is characteristic of Se-O stretching in selenites, whereas in selenates the strong Se-O stretching absorption is around 895 cm^{-1} (Sathianandan et al., 1964). The infrared spectrum of francisite contained no absorption bands attributable to H₂O or OH.

TABLE 1. Electron microprobe analyses of francisite

	1*	2**	3†
	wt%		Atom proportions
CuO	32.62 (32.25–32.96)	33.10	3.10
Bi ₂ O ₃	35.75 (34.98–36.99)	32.31	1.16
SeO ₂	27.23 (26.98–27.75)	30.78	1.86
Cl	4.11 (4.05–4.22)	4.92	0.88
Less O = Cl	0.93	1.11	
Total	98.78	100.00	

* Francisite, Iron Monarch, South Australia. Average of seven analyses, ranges given in parentheses.

** $Cu_3Bi(SeO_3)_2O_2Cl$.

† Francisite, Iron Monarch, South Australia. Atomic proportions calculated such that O + Cl = 9.

TABLE 3. Crystal data and results of crystal-structure refinement for francisite

Crystal size	0.113 × 0.021 × 0.013 mm
Unit-cell dimensions	
<i>a</i> (Å)	6.354(1)
<i>b</i> (Å)	9.630(1)
<i>c</i> (Å)	7.220(2)
<i>V</i> (Å ³)	441.80(2)
<i>Z</i>	2
<i>D_c</i> (g cm ⁻³)	5.42
<i>μ</i> (cm ⁻¹)	354.36
Radiation MoK α	0.7107 Å
Collection limit 2 θ (MoK α)	60°
Unique reflections	734
Reflections <i>I</i> > 3 σ (<i>I</i>)	434
<i>R</i>	0.0443
<i>R_w</i>	0.0395
Δ residual (e Å ⁻³)	
+	3.92
-	3.38

The infrared spectrum is in full accord with the crystal chemistry revealed by the structure determination.

CRYSTAL STRUCTURE

Experimental

Crystal data were obtained using a Philips PW 1100 four-circle diffractometer. Lattice parameters (Table 3) were refined using angles obtained from 24 reflections with 30° < 2 θ < 34°.

TABLE 2. Powder X-ray diffraction data for francisite

<i>hkl</i>	<i>d_{obs}</i> (Å)	<i>d_{calc}</i> (Å)	<i>hkl</i>
20	5.81	5.78	011
60	5.31	5.31	110
100	3.39	3.39	121
30	3.18	3.18	200
5	3.11	3.14	102
15	2.988	2.986	112
15	2.911	2.909	201
15	2.888	2.890	022
80	2.866	2.866	130
5	2.786	2.785	211
70	2.652	2.653	220
60	2.491	2.490	221
25	2.408	2.408	040
5	2.386	2.386	202
5	2.285	2.285	041
10	2.244	2.245	132
5	2.155	2.156	231
10	2.150	2.150	141
10	2.136	2.138	222
30	2.069	2.069	310
10	1.872	1.873	321
10	1.863	1.862	051
10	1.795	1.796	312
25	1.768	1.768	330
35	1.695	1.695	242
15	1.605	1.606	060
60	1.588	1.588	332
20	1.433	1.433	260
15	1.391	1.392	422
15	1.335	1.336	063
20	1.325	1.325	432
5	1.259	1.260	361
5	1.211	1.212	521
5	1.208	1.209	451

Note: Cell parameters refined from the data above: *a* = 6.356(1) Å, *b* = 9.633(2) Å, *c* = 7.224(2) Å. Volume = 442.4(2) Å³.

On the basis of systematic extinctions (*h**h*0, *h* + *k* = 2*n* + 1), space groups *Pm**mn* and *Pm*2₁*n* are permitted; *Pm**mn* was confirmed by refinement. The Bi atom was located using the Patterson method, and subsequent difference-Fourier syntheses revealed the remaining atoms. Weighted least-squares refinement was undertaken using neutral-atom scattering factors with corrections for anomalous dispersion (Cromer and Weber, 1974). Table 3 reports details of data measurement and structure refinement.

The final list of observed and calculated structure factor amplitudes is given in Table 4.¹ The final atomic parameters and their estimated standard deviations are given in Table 5.

¹ A copy of Table 4 may be ordered as Document Am-90-442 from the Business Office, Mineralogical Society of America, 1130 Seventeenth Street NW, Suite 330, Washington, DC 20036, U.S.A. Please remit \$5.00 in advance for the microfiche.

TABLE 5. Final atomic coordinates and thermal parameters for francisite

Atomic coordinates and equivalent isotropic thermal parameters (Å ²)				
	<i>x</i>	<i>y</i>	<i>z</i>	<i>U</i> (eq)
Bi	¼	¼	0.2416(2)	0.0071(3)*
Cu(1)	0	0	0	0.0131(7)*
Cu(2)	¼	¼	0.7922(5)	0.0137(12)*
Se	¼	0.5570(2)	0.6096(3)	0.0076(6)*
Cl	¼	¾	0.1488(14)	0.0330(33)*
O(1)	¼	0.1113(14)	0.9941(21)	0.0074(29)
O(2)	0.0409(16)	0.5836(10)	0.7552(16)	0.0157(21)
O(3)	¼	0.1173(17)	0.5872(23)	0.0169(37)

Anisotropic thermal parameters (Å ² × 10 ⁴)						
	<i>U</i> ₁₁	<i>U</i> ₂₂	<i>U</i> ₃₃	<i>U</i> ₂₃	<i>U</i> ₁₃	<i>U</i> ₁₂
Bi	66(5)	64(5)	82(6)	0	0	0
Cu(1)	116(3)	55(12)	123(13)	-69(12)	41(13)	-87(11)
Cu(2)	322(25)	61(16)	27(21)	0	0	0
Se	72(10)	64(10)	92(11)	8(8)	0	0
Cl	474(68)	345(54)	172(46)	0	0	0

* *U*(eq) = 1/3 Σ_i(*U*_{ii}*a*_i²)

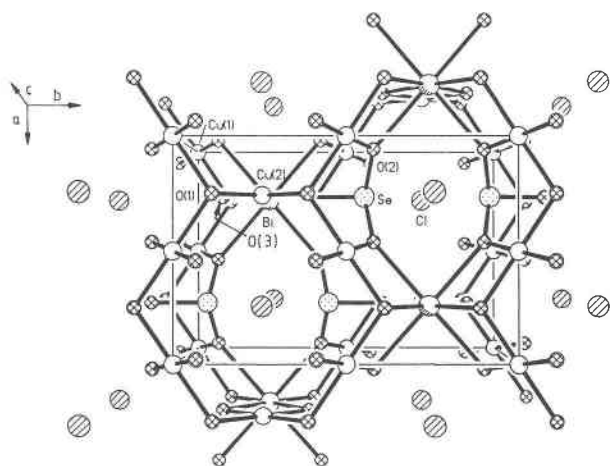


Fig. 3. A diagram of francisite viewed along [001]. Unique atoms are labeled as in Table 5. [Diagram drawn using SHELXTL PLUS (Sheldrick, 1988).]

Structure description

The structure of francisite is depicted in Figure 3; the atomic arrangement consists of an infinite, three-dimensional cation and O framework containing eight-coordinate Bi^{3+} , four-coordinate Cu^{2+} and three-coordinate Se^{4+} ions. The coordination of each ion is illustrated in Figure 4. Chlorine ions and the lone pair of electrons of Se occupy tunnels within the framework parallel to [001].

The Bi ion coordination polyhedron is best described as an 8,14,8- D_{2h} polyhedron, using the method of King (1970), in which the three numbers refer to the number of vertices, edges, and faces of the polyhedron, respectively. King also refers to the polyhedron in terms of 2, 4, and 2 stacked parallel planes of anions, in this case O ions. The Bi-O distances (Table 6) range from 2.23–2.80 Å, with a mean distance of 2.48 Å. The eight O ions of the Bi polyhedron bridge to four Cu(1) atoms, to two

TABLE 6. Bond distances (Å) and angles (°) in francisite

Bonds at Bi		
$\text{Bi}^{\text{A}}-\text{O}(1)^{\text{B}}$ ($\times 2$)	2.23(2)	
$-\text{O}(2)^{\text{D}}$ ($\times 4$)	2.45(1)	
$-\text{O}(3)^{\text{A}}$ ($\times 2$)	2.80(2)	
Mean	2.48	
$\text{Bi}^{\text{A}} \cdots \text{Cu}(2)^{\text{E}}$	3.245(4)	
Angle at Bi		
$\text{O}(1)^{\text{B}}-\text{O}(1)^{\text{C}}$	2.67(3)	73.5(7)
$\text{O}(1)^{\text{A}}-\text{O}(2)^{\text{D}}$ ($\times 4$)	3.92(2)	113.6(3)
$\text{O}(1)^{\text{A}}-\text{O}(2)^{\text{E}}$ ($\times 4$)	2.60(2)	67.4(3)
$\text{O}(1)^{\text{A}}-\text{O}(3)^{\text{A}}$ ($\times 2$)	4.28(2)	116.1(5)
$\text{O}(1)^{\text{A}}-\text{O}(3)^{\text{H}}$ ($\times 2$)	5.02(2)	170.4(5)
$\text{O}(2)^{\text{A}}-\text{O}(2)^{\text{E}}$ ($\times 2$)	4.89(2)	178.9(5)
$\text{O}(2)^{\text{A}}-\text{O}(2)^{\text{F}}$ ($\times 2$)	3.70(2)	98.1(5)
$\text{O}(2)^{\text{A}}-\text{O}(2)^{\text{G}}$ ($\times 2$)	3.21(2)	81.9(5)
$\text{O}(2)^{\text{A}}-\text{O}(3)^{\text{A}}$ ($\times 4$)	4.22(2)	106.9(3)
$\text{O}(2)^{\text{A}}-\text{O}(3)^{\text{H}}$ ($\times 4$)	3.10(2)	72.1(3)
$\text{O}(3)^{\text{A}}-\text{O}(3)^{\text{H}}$	2.56(3)	54.2(7)
Bonds at Cu(1)		
$\text{Cu}(1)^{\text{A}}-\text{O}(1)^{\text{B}}$ ($\times 2$)	1.917(8)	
$-\text{O}(2)^{\text{C}}$ ($\times 2$)	1.96(1)	
Mean	1.939	
$\text{Cu}(1)^{\text{A}} \cdots \text{Cl}^{\text{I}}$ ($\times 2$)	3.078(4)	
Angle at Cu		
$\text{O}(1)^{\text{B}}-\text{O}(1)^{\text{J}}$	3.83(2)	180.0(—)
$-\text{O}(2)^{\text{C}}$	2.87(2)	95.7(5)
$-\text{O}(2)^{\text{E}}$	2.60(2)	84.3(5)
Bonds at Cu(2)		
$\text{Cu}(2)^{\text{A}}-\text{O}(3)^{\text{H}}$ ($\times 2$)	1.96(2)	
$-\text{O}(1)^{\text{B}}$ ($\times 2$)	1.98(2)	
Mean	1.97	
$\text{Cu}(2)^{\text{A}} \cdots \text{Cl}^{\text{I}}$ ($\times 2$)	3.206(1)	
Angle at Cu		
$\text{O}(3)^{\text{H}}-\text{O}(3)^{\text{K}}$	2.56(3)	81.6(9)
$\text{O}(3)^{\text{H}}-\text{O}(1)^{\text{B}}$	2.94(2)	96.7(6)
$\text{O}(3)^{\text{H}}-\text{O}(1)^{\text{J}}$	3.93(2)	178.3(7)
Bonds at Se		
$\text{Se}^{\text{A}}-\text{O}(3)^{\text{H}}$	1.69(2)	
$-\text{O}(2)^{\text{D}}$ ($\times 2$)	1.71(2)	
Mean	1.70	
$\text{Se}^{\text{A}} \cdots \text{Cu}(2)^{\text{A}}$	3.237(3)	
Angle at Se		
$\text{O}(3)^{\text{H}}-\text{O}(2)^{\text{D}}$ ($\times 2$)	2.64(2)	102.0(5)
$\text{O}(2)^{\text{A}}-\text{O}(2)^{\text{D}}$	2.66(2)	101.7(7)

Note: (A) x, y, z ; (B) $x, y, z - 1$; (C) $x, \frac{1}{2} - y, z - 1$; (D) $-x, 1 - y, 1 - z$; (E) $\frac{1}{2} + x, y - \frac{1}{2}, 1 - z$; (F) $\frac{1}{2} + x, 1 - y, 1 - z$; (G) $-x, y - \frac{1}{2}, 1 - z$; (H) $x, \frac{1}{2} - y, z$; (I) $-x, -y, 1 - z$; (J) $x, y - 1, z$; (K) $-x, 1 - y, -z$; (L) $1 - x, 1 - y, 1 - z$; (M) $\frac{1}{2} - x, y, z$.

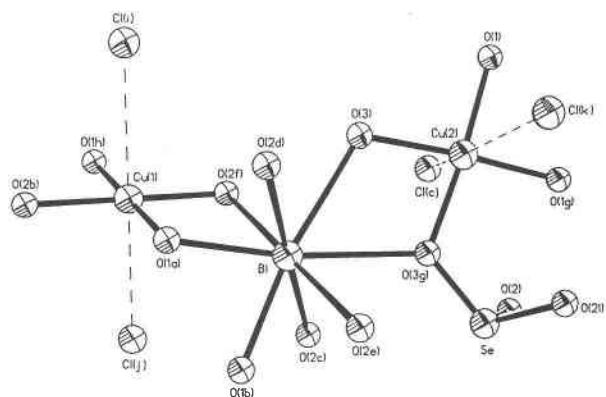


Fig. 4. A diagram showing the O and Cl coordination of the Bi, Cu(1), Cu(2), and Se atoms. Small letters in parentheses correspond to the symmetry transformations indicated in capital letters at the bottom of Table 6. [Diagram drawn using SHELXTL PLUS (Sheldrick, 1988).]

Cu(2) atoms, and to two Se atoms. The angles subtended by pairs of O ions at Bi and the O-O distances are listed in Table 6.

The two independent Cu ions are both square-planar in their coordination; Cu(1)-O distances range from 1.917–1.96 Å (mean 1.939 Å) and Cu(2) 1.96–1.98 Å (mean 1.97 Å); angles subtended at Cu by pairs of O ions and the O-O distances are given in Table 6. It is evident from Figure 3 that the Cu(1) square planes have one O in common, O(1), that links them into a zig-zag chain parallel to [100]. The angle between successive square planes is 117.8°. These chains are reflected in the mirror plane at $y = \frac{1}{4}$, on which the Bi, Cu(2), and Cl ions are located. The Cu(2) ions link the Bi coordination polyhedra along [001]. In $\text{Cu}_3\text{Se}_2\text{O}_8\text{Cl}_2$ (Galy et al., 1979) Cu occurs in three coordinations; the square-planar arrangement of one Cu in this structure is similar to that in francisite, with a mean Cu-O distance of 1.961 Å compared with the mean Cu-O distance in francisite of 1.955 Å. However, the Cu-

Cl distances of this Cu in $\text{Cu}_5\text{Se}_2\text{O}_8\text{Cl}_2$, 2.957 Å, are somewhat shorter than the mean Cu-Cl distance reported here for francisite (3.142 Å).

The Se ions are three-coordinate in a triangular pyramidal arrangement with a mean Se-O distance of 1.70 Å; the Se-O bond lengths are typical of those in other selenites (e.g., Kohn et al., 1976; Galy et al., 1979; Effenberger, 1986; Effenberger and Pertlik, 1986; Hawthorne et al., 1986; Effenberger, 1988). The position of the stereochemically active lone pair of electrons of Se was calculated as being at the apex of the tetrahedron whose base is formed by the three O ions coordinated to Se. From Figure 4 it can be seen that the lone pair is located in the tunnel that the Cl ions occupy. The structure of $\text{Cu}_5\text{Se}_2\text{O}_8\text{Cl}_2$ (Galy et al., 1979) is described as having a Cl ion, and the lone pair of a Se atom (E) located in an O polyhedron with 15 vertices in which the E-Cl distance is given as ~2.10 Å. The possibility of some interaction between the lone pair and the large anion was suggested. The E-Cl distance in francisite of ~2.51 Å, calculated using the same Se-E distance as Galy et al., (1979) of ~1.3 Å, could indicate a further example of such an interaction.

PARAGENESIS

Francisite appears to have formed from the oxidation of the primary copper and bismuth selenides and sulfides that occur with it, probably through the action of low temperature hydrothermal fluids. It is known that the Fe-Mn ore contains significant amounts of elements such as Cu, Zn, As, and P, which have been sufficiently concentrated to give rise to suites of locally abundant secondary minerals such as atacamite, turquoise, pseudomalachite, faustite (Segnit and Francis, 1983), kleemanite (Pilkington et al., 1979), arsenoklasite, pyrobelonite, and switzerite (Pring et al., 1989). The formation of francisite therefore seems likely to have been a two-stage process. Small amounts of Se, Bi, Ag, and Cu were leached from the Fe-Mg ore body by Ba- and S-rich fluids, possibly during a low grade metamorphic event associated with the folds, and their constituents were redeposited as inclusions within massive barite. This assemblage was later subjected to oxidation, possibly by Cl-rich ground waters, precipitating francisite and chlorargyrite. Small crystals

of synthetic francisite have been made by hydrothermal methods (Berrigan and Gatehouse, unpublished results).

ACKNOWLEDGMENTS

The assistance of G.D. Fallon in preparation of the figures is gratefully acknowledged. Thanks are also due to Stuart McClure of CSIRO Division of Soils for the SEM photomicrographs and David Tilbrook of the South Australian Conservation Center for the infrared spectrum of francisite.

REFERENCES CITED

- Cromer, D.T., and Weber, J.T. (1974) International tables for X-ray crystallography, vol. IV, Kynoch Press, Birmingham, England.
- Effenberger, H. (1986) Die Kristallstrukturen von drei Modifikationen des $\text{Cu}(\text{SeO}_3)$. *Zeitschrift für Kristallographie*, 175, 61-72.
- (1988) Contribution to the stereochemistry of copper. The transition from a tetragonal pyramidal to a trigonal bipyramidal $\text{Cu}(\text{II})\text{O}_3$ coordination figure with a structure determination of $\text{PbCu}_2(\text{SeO}_3)_3$. *Journal of Solid State Chemistry*, 73, 118-126.
- Effenberger, H., and Pertlik, F. (1986) Die Kristallstrukturen der Kupfer(II)-oxo-selenite $\text{Cu}_2\text{O}(\text{SeO}_3)$ (kubisch und monoklin) und $\text{Cu}_4\text{O}(\text{SeO}_3)_3$ (monoklin und triklin). *Monatshefte für Chemie*, 117, 887-896.
- Galy, J., Bonnet, J.-J., and Andersson, S. (1979) The crystal structure of a new oxide chloride of copper(II) and selenium (IV): $\text{Cu}_5\text{Se}_2\text{O}_8\text{Cl}_2$. *Acta Chemica Scandinavica*, A33, 383-389.
- Hawthorne, F.C., Ercit, T.S., and Groat, L.A. (1986) Structures of zinc selenite and copper selenite. *Acta Crystallographica*, C42, 1285-1287.
- King, R.B. (1970) Chemical applications of group theory IV. *Journal of the American Chemical Society*, 92, 6460-6466.
- Kohn, K., Inoue, K., Horie, O., and Akimoto, S-I. (1976) Crystal chemistry of MSeO_3 and MTeO_3 (M = Mg, Mn, Co, Ni, Cu, and Zn). *Journal of Solid State Chemistry*, 18, 27-37.
- Milnes, K. R. (1954) The geology and iron ore resources of the Middleback Range Area. *Geological Survey of South Australia, Bulletin 33*, 245 p.
- Pilkington, E.S., Segnit, E.R., and Watts, J. (1979) Kleemanite, a new zinc aluminium phosphate. *Mineralogical magazine*, 43, 93-95.
- Pring, A., Francis, G. L., and Birch, W. D. (1989) Pyrobelonite, arsenoklasite, switzerite and other recent finds at Iron Monarch, South Australia. *Australian Mineralogist*, 4, 49-55.
- Sathianandan, K., McCarty, L.D., and Margrave, J.L. (1964) Infrared absorption spectra of inorganic solids-III selenites and selenates. *Spectrochimica Acta*, 20, 957-963.
- Segnit, E.R., and Francis, G.L. (1983) Secondary phosphate minerals from Iron Monarch South Australia. *Australian Mineralogist*, 1, (43), 243-250.
- Sheldrick, G.M. (1976) SHELX76, Program for crystal structure determination. Cambridge University, Cambridge, United Kingdom.
- (1988) SHELXTL PLUS, Revision 3.4, Siemens Analytical X-Ray Instruments, Inc., Madison, Wisconsin, U.S.A.

MANUSCRIPT RECEIVED JANUARY 2, 1990

MANUSCRIPT ACCEPTED SEPTEMBER 28, 1990